

Vector Control for an Interior Permanent Magnet Synchronous Machine with Maximum Torque per Ampere Strategy

Dominguez X.*; Imbaquingo C.**

*Escuela Politécnica Nacional, Facultad de Ingeniería Eléctrica y Electrónica, Quito, Ecuador
e-mail: xavier.dominguez@epn.edu.ec

** Escuela Politécnica Nacional, Facultad de Ingeniería Eléctrica y Electrónica, Quito, Ecuador
e-mail: carlos.imbaquingo@epn.edu.ec

Resumen: El principal objetivo de este artículo es detallar una metodología para implementar una estrategia de control de Máximo Torque por Amperio (MTPA) en una Máquina Síncrona de Imanes Interiores Permanentes (IPMSM). Las IPMSMs han sido ampliamente usadas en los últimos años en la industria al presentar un excelente desempeño dinámico y una alta densidad de poder. En el presente estudio, criterios y teoría de la estrategia MTPA y control vectorial son detallados en primer lugar. Luego, el análisis matemático y aspectos de simulación son presentados. Finalmente, el comportamiento del control de velocidad y torque es expuesto. Los resultados muestran respuestas exitosas del sistema en estado estable y durante transitorios.

Palabras clave: Control de velocidad, Control vectorial, IPMSM, MTPA, Referencia síncrona

Abstract: The main objective of this paper is to show a methodology to implement a Maximum Torque per Ampere Strategy (MTPA) in an Interior Permanent Magnet Synchronous Machine (IPMSM). IPMSM's have been broadly used on industry in the last years for having excellent dynamic performance and high power density. In this article, vector control and MTPA theory and criteria are firstly detailed. Then, the mathematical analysis and simulation aspects are presented. Lastly, the speed and torque control responses are exposed. The results show successful responses of the system on steady-state and during transients.

Keywords: IPMSM, MTPA, speed control, synchronous frame, vector control

1. INTRODUCTION

The permanent-magnet synchronous motor (PMSM) has received notorious acceptance in industrial applications due to its high efficiency, high torque-current ratio, low noise, and robustness [1][2][3]. In particular, the interior PMSM (IPMSM) provides a smooth rotor surface and better dynamic performance [4]. In order to make appropriate use of these relevant advantages in this machine, the use and application of an accurate and efficient control technique needs to be developed and tested; this precisely the purpose of this paper. This goal will be achieved with the use of the Maximum Torque per Ampere (MTPA) strategy [5] and vector control theory.

For simulation and analysis purposes of the IPMSM control, common electrical parameters for this kind of machine analyzed by references [6] [7] will be assumed as Table 1 details.

2. VECTOR CONTROL USING MTPA TECHNIQUE

The synchronous reference frame will be implemented by the use of Park transformations [8] so that we can transform a 3-

phase system into dq components (Equation 1). This will be especially helpful when controlling stator currents because instead of tracking three 50/60 Hz sinusoidal reference signals (I_a , I_b , I_c) only two DC reference signals will need to be tracked (the quadrature and direct currents, I_q and I_d respectively). On the other hand, dq to abc transformation (See Equation 2) is useful when feeding back voltage references to the machine as three phase values are again required.

Table 1. IPM Parameters

PARAMETER	SYMBOL	VALUE
Stator resistance	R_s	0.43 Ω
D-axis stator inductance	L_d	27 mH
Q-axis stator inductance	L_q	67 mH
No-load peak line-to-line voltage constant	V_{pk}/k_{rpm}	98.67 V (peak value @ 1000rpm)
Number of pole pairs	p	2
Moment of inertia	J	0.00179 kg*m ²
Rated current	I_n	10A
Mechanical Load Torque	K_l	0.00764 Nm/(rad/s)

$$\begin{bmatrix} V_{qs} \\ V_{ds} \\ V_0 \end{bmatrix} = \begin{bmatrix} \frac{2}{3} * \cos(\theta) & \frac{2}{3} * \cos(\theta - 2\pi/3) & \frac{2}{3} * \cos(\theta + 2\pi/3) \\ \frac{2}{3} * \sin(\theta) & \frac{2}{3} * \sin(\theta - 2\pi/3) & \frac{2}{3} * \sin(\theta + 2\pi/3) \\ 1/3 & 1/3 & 1/3 \end{bmatrix} \begin{bmatrix} V_{as} \\ V_{bs} \\ V_{cs} \end{bmatrix} \quad (1)$$

$$\begin{bmatrix} V_{as} \\ V_{bs} \\ V_{cs} \end{bmatrix} = \begin{bmatrix} \cos(\theta) & \sin(\theta) & 1 \\ \cos(\theta - 2\pi/3) & \sin(\theta - 2\pi/3) & 1 \\ \cos(\theta + 2\pi/3) & \sin(\theta + 2\pi/3) & 1 \end{bmatrix} \begin{bmatrix} V_{qs} \\ V_{ds} \\ V_0 \end{bmatrix} \quad (2)$$

To successfully achieve the MTPA condition, the synchronous reference frame with the dq axes placed like in Fig. 1 will be considered. There we can see that the q axis is ahead the a axis with the θ_e angle ($\theta_e = \theta$). Additionally, it can be observed the q and d axes being in quadrature and rotating at an angular speed equal to ω_e . Therefore in this quadrature reference, the current only has direct (I_d) and quadrature (I_q) components.

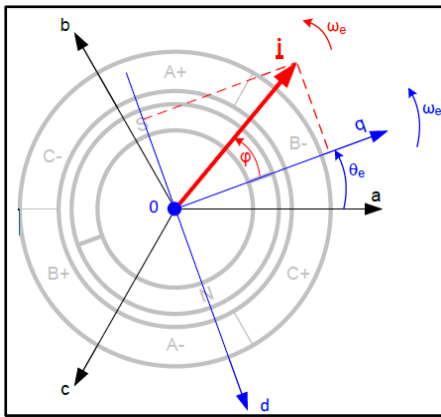


Figure 1. Selection of the d-q axes positions

For the assumed dq scheme, the torque and current in a PMSM are related with Equations 3 to 6 [8][9]:

$$T = 1.5 P (\lambda_{pm} I_q + (L_d - L_q) I_d I_q) \quad (3)$$

$$I_q = I \cdot \cos(\varphi) \quad (4)$$

$$I_d = -I \cdot \sin(\varphi) \quad (5)$$

$$I = \sqrt{I_q^2 + I_d^2} \quad (6)$$

Where λ_{pm} is the amplitude of the permanent magnet machine flux linked to the stator windings, while L_d and L_q are the direct and quadrature inductances respectively. By using Equation 7 [10] and considering the figures in Table 1, for this study case, λ_{pm} is found to be equal to 0.272 [V.s].

$$\lambda_{pm} = \frac{60 * V_{pk} / k_{rpm}}{2 * \sqrt{3} * \pi * P * 1000} \quad (7)$$

Contrary to the Surface Permanent Magnet Synchronous Machine (SPMSM) [9][11] where the direct current is set to be null, in the IPMSM the direct and quadrature currents need to be both appropriately controlled to produce the desired current module (I) and thus the required torque. However, there is an infinite number of I_q and I_d currents combinations which may produce the same final current module as Equation 6 implies. This is reason why the MTPA control strategy seeks to maximize the torque for a given amount of current by maximizing the torque function with respect to the φ angle ($\frac{d}{d\varphi} T = 0$). If we do this after replacing Equations 4 and 5 in 3, we have:

$$\frac{3}{2} P (-\lambda_{pm} I \sin(\varphi) - I^2 (L_d - L_q) \cos(2\varphi)) = 0 \quad (8)$$

When solving Equation 8 for φ and considering the nominal current $I = I_{nominal} = 10$ [A] (Table 1); from the obtained mathematical answers the angle that produces the biggest torque is $\varphi = 33.86^\circ$ with 12.32 [Nm]. For this condition and using Equations 4 and 5, we obtain $I_q = 8.303$ [A] and $I_d = -5.57$ [A].

In Fig. 2 it can be visualized the I_d and I_q components relation in MTPA conditions for different current amplitudes (I) between 1 and 10 [A]. As we can see, the bigger I_q the bigger the negative I_d . As permanent magnets present higher reluctance than iron, the inductance along the d axis tends to be smaller than the one on the q -axis [15]. For these reason in typical IPMSMs, L_d is lower than L_q . This results on the need of introducing negative I_d to produce positive torque on the d axis.

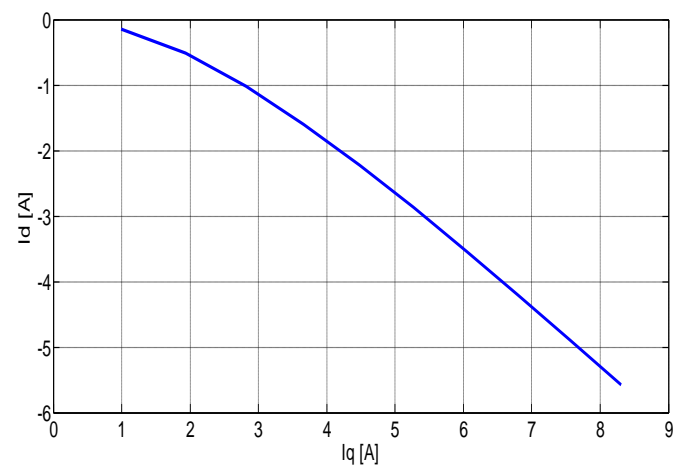


Figure 2. I_d vs I_q in MTPA condition

Using the previous I_d and I_q values for the MTPA case, the back-emf voltage values (EMF) on q and d axes can be obtained by the use of the following equations [8][9]:

$$EMFq = We (\lambda pm + Ld.Id) \quad (9)$$

$$EMFd = -We.Lq.Iq \quad (10)$$

$$We = P.Wr \quad (11)$$

Where We and Wr are the electrical and mechanical speeds of the rotor respectively. If we plot $EMFd$ vs $EMFq$, it can be observed in Fig. 3 the inverse relation between their amplitudes. The bigger the $EMFq$, the lower the $EMFd$ module. This can be explained as the $EMFd$ depending on q -axis variables and vice versa, as Equations 9 and 10 imply.

To implement the MTPA strategy, Equation 6 is replaced in 3 so that we can get Id in function of Iq as we can see in Equation 12.

$$Id = -\frac{\lambda pm}{2(Ld-Lq)} - \sqrt{\frac{\lambda pm^2}{4(Ld-Lq)^2} + Iq^2} \quad (12)$$

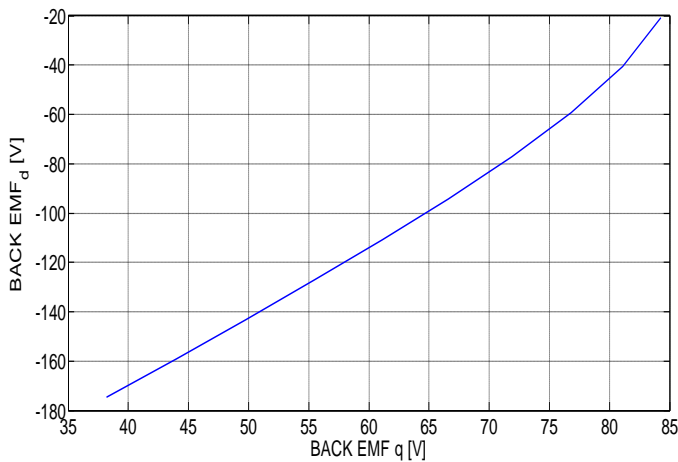


Figure 3. BACK_EMFd vs BACK_EMFq in MTPA condition

Then, replacing Equation 12 in 3 we finally have:

$$T = \frac{3}{2} P \left[\frac{1}{2} \lambda pm.Iq - (Ld - Lq) \sqrt{\frac{\lambda pm^2.Iq^2}{4(Ld-Lq)^2} + Iq^4} \right] \quad (13)$$

Now, we need to bear in mind that the reference torque is the input of the system (as it depends from the machine's load) while Iq is the output. As in the previous Equation it is not simple to mathematically isolate Iq , we can give appropriate values to Iq to get their corresponding torque T components. If we do this we can plot Iq versus T as in Fig. 4 so that we could use a curve fitting method [12] to finally obtain an expression for Iq in function of the required torque T . To get enough accuracy when doing this procedure, a fifth polynomial degree curve for the fitting process was used (Equation 14). This mathematical approximation model presented a 95% of confidence bounds with a Root Mean

Squared Error (RMSE) of 1.65%. In fact, the fitting curve is very accurate as we can clearly observe in Fig. 5 where a deep zoomed area from the non-linear part of the original plot (Fig. 4) has been made.

$$Iq = a.T^5 + b.T^4 + c.T^3 + d.T^2 + e.T + f \quad (14)$$

Table 2. Fitting curve constants values

CONSTANT	VALUE
a	1.448E-6
b	-0.0001314
c	0.00469
d	-0.08753
e	1.249
f	0.02338

However, it must be mentioned that for the MTPA technique to work properly, the parameters of the machine (λpm , Ld , Lq) should not vary on time [13][14]. This is why it is very critical to provide nominal operation conditions for the motor as well to successfully control its temperature. Lastly, for a given required torque only Id is missing and it can be obtained by means of Equation 12.

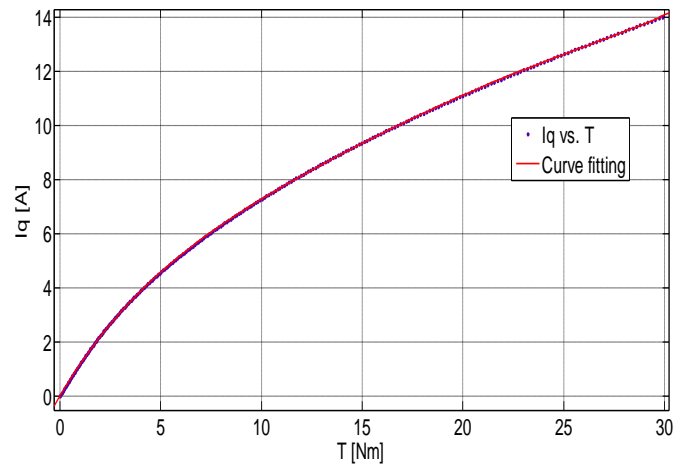


Figure 4. Iq vs T with equation (12) and curve fitting

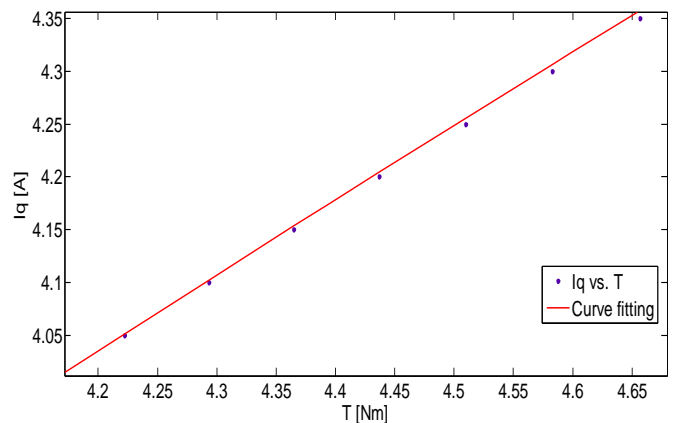


Figure 5. Iq vs T deep zoom with equation (12) and curve fitting

3. TORQUE CONTROL TOPOLOGY

The inner loop shown in the block diagram detailed in Fig. 6 has been used to perform the torque control of the IPMSM. The implementation of the torque control using PSIM® Software, including the control and power stages, is the one exposed in detail in Figs 7 and 8.

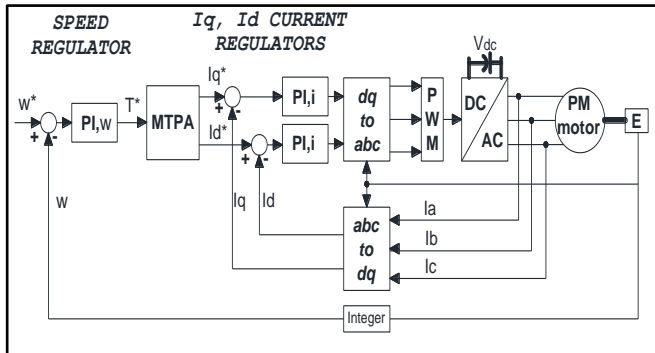


Figure 6. Torque control with MTPA strategy scheme

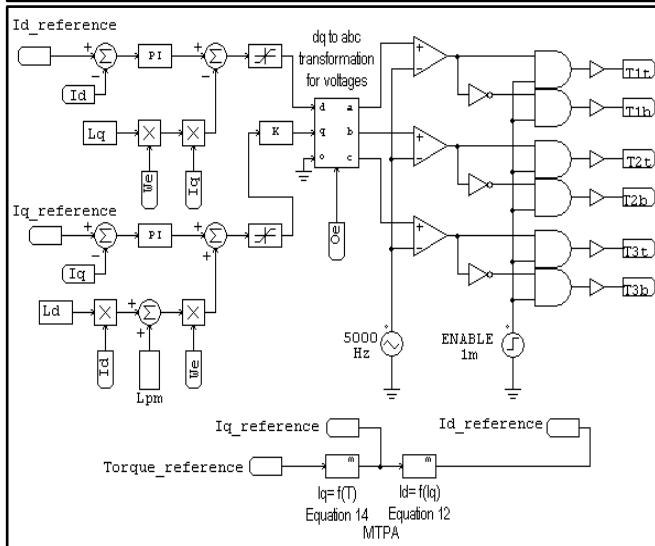
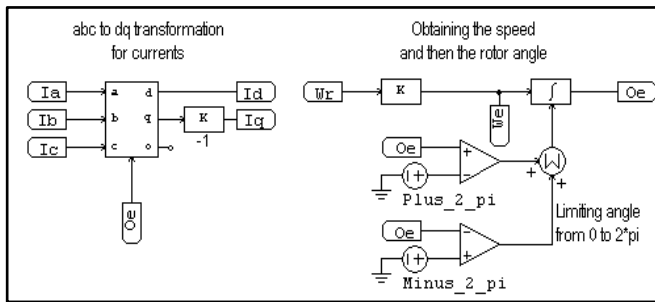


Figure 7. Torque control with MTPA strategy implemented in PSIM®

For the design of the I_q and I_d regulators, the selected closed loop bandwidth was 100 [Hz]. The closed loop structure is shown in Fig. 9, being L and R , the per-phase inductance and resistance of the motor. However, for the I_q and I_d regulators we consider L_q and L_d respectively for the design of the PI

controllers in Equations 15 and 16. Thus, we get for the I_q controller $K_p=42.09$ with $K_i=6.41$, while for the I_d controller it was attained $K_p=16.96$ and $K_i=15.92$.

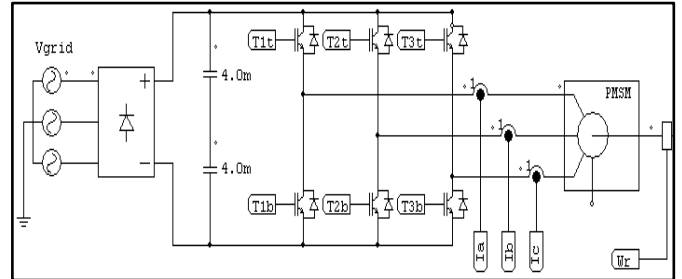


Figure 8. Power stage in PSIM® to achieve the MTPA strategy

$$K_p = 2 \cdot \pi \cdot \text{Bandwidth}_{\text{Hz}} \cdot L \quad (15)$$

$$K_i = R_s/L \quad (16)$$

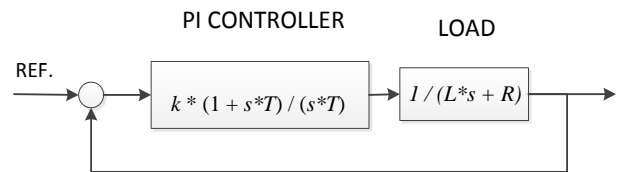


Figure 9. Closed loop PI Regulator scheme

To confirm a successful action of the controllers, we can verify the response time (T_r) of the closed loop system which is the necessary time for the controlled variable to reach 63% of the commanded reference on a first order system. When the requested torque is 10 [Nm], I_q and I_d references in MTPA condition are set to 7.281 [A] and -4.635 [A] respectively. So, the 63% of the I_q reference is $0.63 \cdot 7.281 = 4.58$ [A].

As in the PSIM® model the IGBT's gate signals are enabled at 1 [ms], in Fig. 9 it can be confirmed that T_r is equal to 1.562 [ms] and it is the required time to reach 4.58 [A].

Now, considering control theory we could verify the bandwidth of the system by using Equation 17. Replacing the T_r obtained previously with the simulator, we get the bandwidth equal to 101.89 [Hz] which is practically the desired value.

$$\text{Bandwith [Hz]} = 1 / (2 \cdot \pi \cdot T_r) \quad (17)$$

Additionally, if we plot a Bode diagram for the system as in Fig. 11, it can be checked that with a magnitude of -3 [dB] the closed loop frequency response of the system is equal to 99.7 [Hz] which is again in a practical way the required value.

This fact again corroborates an appropriate design of the controllers.

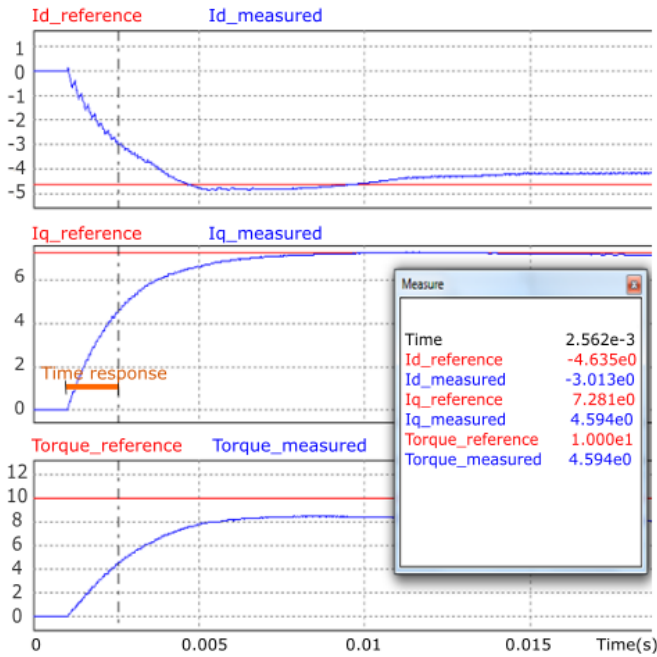


Figure 10. Closed loop time response T_r for current regulators

5.54 [A] and $I_d = -6.61$ [A]. Replacing these values as well as the initially considered parameters of the machine in Equation 3, we obtain that the torque is equal to 8.91 [Nm]; which is a lower value than the one obtained with MTPA (10 [Nm]). It can be verified for different φ angles that the only one producing MTPA condition was the one achieved by means of the detailed methodology.

On the other hand, when talking about the response of the system, it must be mentioned that initially, the back-emf effect was neglected in the controllers. However, this produced an unwanted response on I_d especially as Fig. 12 reveals. After implementing back-emf compensation for the I_q and I_d current controllers, the I_d current and torque responses were improved as Fig. 13 reveals.

4. SPEED CONTROL LOOP FOR THE IPMSM

Once the current controllers behave properly, the speed control loop (outer loop in Fig. 6) will be implemented with the same procedure used for the current regulators. The closed loop system has the same configuration as the one in Fig. 9, however this time the transfer function of the plant to be controlled is:

$$G(s) = \frac{1}{(J + J_{load})s + (B + K_1)} \quad (18)$$

Where, J and J_{load} are the machine's and load's moment of inertia respectively. J_{load} will be considered equal to 0.030 [kg.m²] while B , which is the friction coefficient of the machine will be obtained as Equation 19 exposes. There, τ_{mech} is the mechanical time constant of the machine and it will be assumed to be equal to 0.3 [s] which is a typical value.

$$\tau_{mech} = \frac{J}{B} \quad (19)$$

For this case the PI constants for the speed regulator will be:

$$K_p = 2 \cdot \pi \cdot Bandwidth_{Hz} \cdot (J + J_{load}) \quad (20)$$

$$K_i = (B + K_1) / (J + J_{load}) \quad (21)$$

Thus, we have $K_p = 0.08765$ and $K_i = 3.379$. Verifying the time response (T_r) for the speed closed loop, we obtain the results exposed in Fig. 14 when requiring a set point rotor speed of 100 rad/s. There it can be verified that T_r is 31.4 [ms] (considering again that IGBT'S are enabled at 1 [ms]). Using Equation 17 the bandwidth of the system would be 5.06 [Hz] which is again in practical terms the desired 5 [Hz] bandwidth.

Several simulations were performed to confirm a good speed response of the system. Proper results were obtained at steady

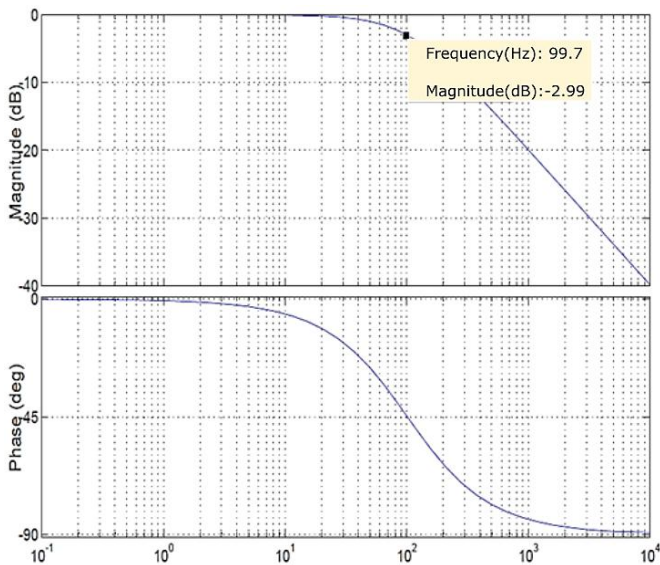


Figure 11. Bode diagram for the closed loop system

In order to briefly test if the MTPA technique was accomplished, we could simply change the phase angle advance (φ) for the current. In MTPA condition, when 10 [Nm] is required, $I_q = 7.281$ [A] and $I_d = -4.635$ [A]. This implies a total current of 8.631 [A] if we use Equation 6, this represents an advance angle $\varphi = 32.48^\circ$.

With the same amount of total current (8.631 [A]), if we change for example the angle φ to 50° , the currents are $I_q =$

state and during transients. In Fig. 15 it can be appreciated a successful system response when 100 [rad/s] were required as a rotor speed reference from zero to 0.2 [ms] and then the reference changed to 40 [rad/s] until 0.4 [ms]. As it can be observed, the proposed control technique presents a suitable dynamic response which is a relevant advantage against schemes based on online search algorithms that show a poor dynamic behavior [15] [16] and undesirable torque disturbance [17]. In PSIM® the employed elements to perform the speed control are exposed in Fig. 16.

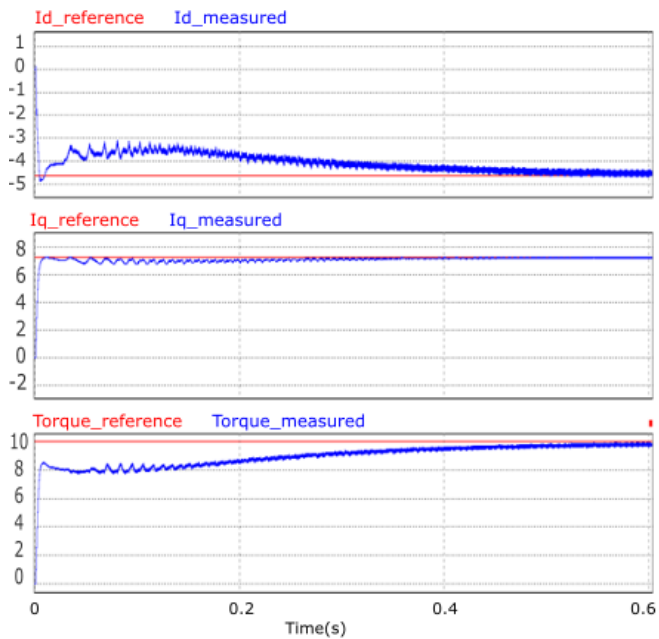


Figure 12. System response without back-emf compensation

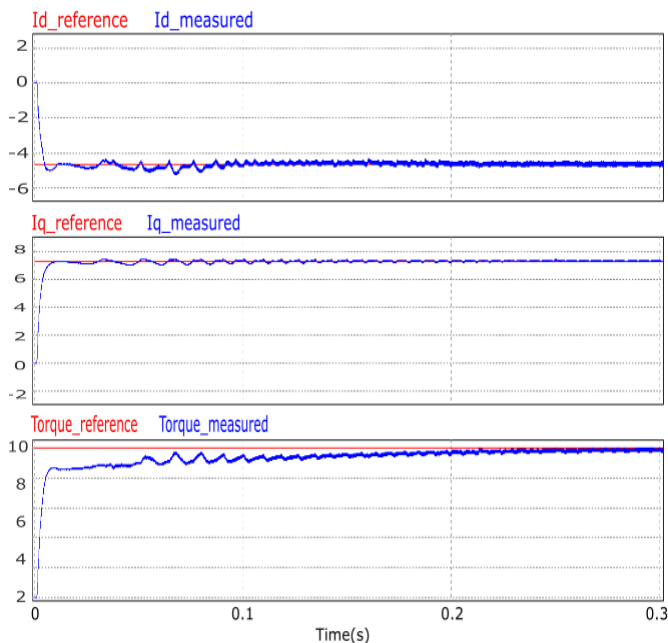


Figure 13. System response with back-emf compensation

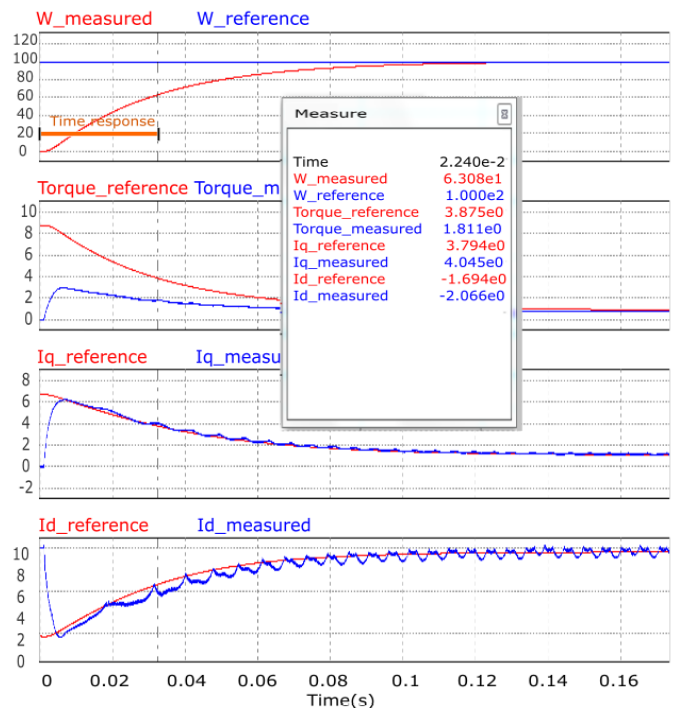


Figure 14. Speed closed loop system response time

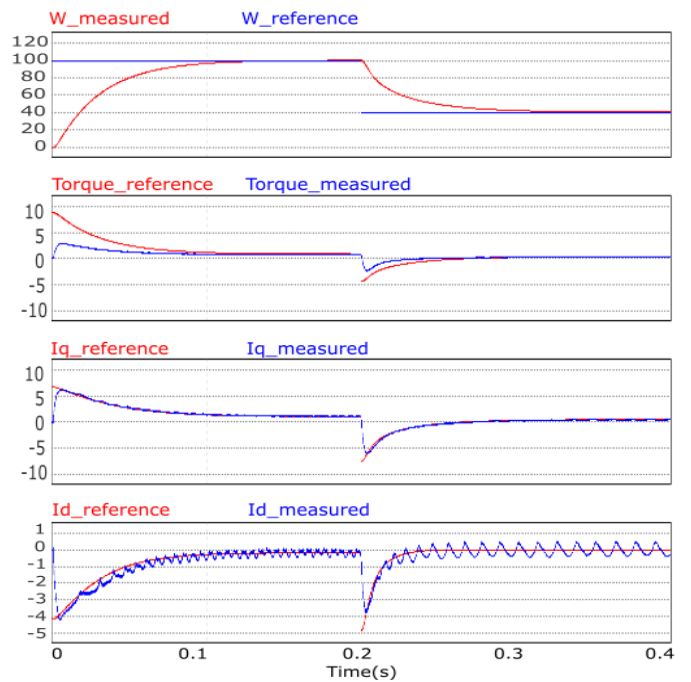


Figure 15. Speed closed loop system response

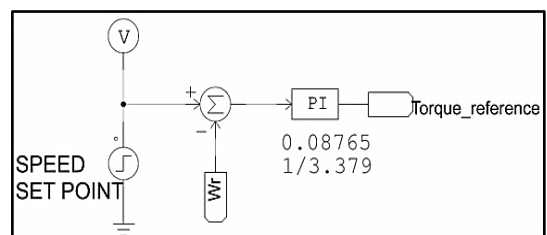


Figure 16. Speed control elements in PSIM®

5. CONCLUSIONS

In this paper, by means of a maximum torque per ampere strategy, a vector control for an IPMSM has been successfully implemented. The use of Park transformations was especially helpful as it permitted to track only two dc reference signals (I_d and I_q) instead of three sinusoidal references. The proposed methodology has been validated by performing several simulation conditions in PSIM® software. Proper speed and torque control responses were attained on steady state and during transients. For the MTPA technique to be effective, nominal operating conditions should be given to the motor (mainly in terms of temperature) so that the parameters of the machine will not vary on time.

6. FUTURE WORK

As a part of future work, it is intended to consider non-linearities regarding the magnetic saturation and unwanted temperature effects of the motor that appear when working with higher current rates. Additionally, to improve the performance of the system, robust algorithms against unexpected parameter variations will be studied and used.

REFERENCES

- [1] Pillay P. and Krishnan R., "Control characteristics and speed controller design of a high performance PMSM," in Proc. IEEE Ind. Appl. Soc.
- [2] Rudnicki, T.; Czerwinski, R.; Frechowicz, A., "Permanent magnet synchronous motor control driver," Mixed Design of Integrated Circuits and Systems, 2011 Proceedings of the 18th International Conference , vol., no.45., pp.545,548, 16-18 June 2011
- [3] Fodorean, D.; Szabo, L., "Control of a permanent magnet synchronous motor for electric scooter application," Power Electronics, Electrical Drives, Automation and Motion, 2012 International Symposium on , vol., no., pp.1178,1181, 20-22 June 2012
- [4] Fang, J.; Heising, C.; Staudt, V.; Steimel, A., "Permanent-Magnet Synchronous Machine model for urban transport applications", Optimization of Electrical and Electronic Equipment, 2010 12th International Conference on , vol., no., pp.358,363, 20-22 May 2010
- [5] Shoudao Huang; Ziqiang Chen; Keyuan Huang; JianGao, "Maximum torque per ampere and flux-weakening control for PMSM based on curve fitting," Vehicle Power and Propulsion Conference (VPPC), 2010 IEEE , vol., no., pp.1,5, 1-3 Sept. 2010
- [6] Odhano, S; Giangrande, P; Bojoi, R., "Self-commissioning of Interior Permanent Magnet Synchronous Motor Drives With High-Frequency Current Injection", IEEE Transactions on Industry Applications, vol, no 50, issue: 5, March 2014
- [7] Hassan, A.and. Azzam, M; "Robust control of a speed sensorless permanentmagnet synchronous motor drive", Faculty of Engineering. El-Minia University, El-Minia, Egypt.
- [8] D.W. Novotny and T.A. Lipo, "Vector Control and Dynamics of AC Drives", Oxford University Press, New York, 1998.B.
- [9] Kitajima, J.; Ohishi, K., "Rapid and stable speed control of SPMSM based on current differential signal," Power Electronics Conference (IPEC-Hiroshima 2014 - ECCE-ASIA), 2014 International , vol., no., pp.1247,1252, 18-21 May 2014
- [10] PSIM User`s guide, Version 9.0, Release 3, May 2010. Available at: www.powersimtech.com
- [11] Maekawa, S.; Hinata, T.; Suzuki, N.; Kubota, H., "Study of low speed sensorless drives for SPMSM by controlling elliptical inductance," Power Electronics Conference (IPEC-Hiroshima 2014 - ECCE-ASIA), 2014 International , vol., no., pp.919,924, 18-21 May 2014
- [12] Guest, P., "Numerical Methods of curve fitting paperback", Cambridge University Press, London, 2012.
- [13] Kim, Sang Min; Kwon, Taesuk, "A simple method to minimize effects of temperature variation on IPMSM control in real-time manner," Energy Conversion Congress and Exposition (ECCE), 2014 IEEE , vol., no., pp.4212,4217, 14-18 Sept. 2014
- [14] Gubae Rang; Jaesang Lim; Kwanghee Nam; Hyung-Bin Ihm; Ho-Gi Kim, "A MTPA control scheme for an IPM synchronous motor considering magnet flux variation caused by temperature," Applied Power Electronics Conference and Exposition, 2004. APEC '04. Nineteenth Annual IEEE , vol.3, no., pp.1617,1621 Vol.3, 2004
- [15] Ahmed, A., "Maximum torque per ampere (MTPA) control for permanentmagnet synchronous machine drive system", Master Thesis, University of Akron, Ohio-USA
- [16] Antonello, R.; Carraro, M.; Zigliotto, M., "Towards the automatic tuning of MTPA algorithms for IPM motor drives," Electrical Machines (ICEM), 2012 h International Conference on , vol., no., pp.1121,1127, 2-5 Sept. 2012

- [17] Mademlis, C.; Kioskeridis, I. and Margaris, N., “Optimal efficiency control strategy for interior permanent-magnet synchronous motor drives,” IEEE Transactions on Energy Conversion, vol. 19, no. 4, pp. 715–723, Dec. 2004.